Phase changes induced by optical aberrations degrade letter and face acuity

Sowmya Ravikumar
Vision Science Program, University of California, Berkeley, CA, USA

Arthur Bradley
School of Optometry, Indiana University, Bloomington, IN, USA

Larry Thibos
School of Optometry, Indiana University, Bloomington, IN, USA

Optical aberrations of the eye reduce image contrast and induce spatial phase shifts in the retinal image. The resulting degradation of retinal image quality hampers recognition of complex objects such as letters and faces. To study the effects of spatial phase shifts on object recognition, we simulated image blur computationally for 4 types of aberrations (defocus, astigmatism, coma, and spherical aberration) present individually or in combinations. Phase errors in the computed images were corrected (by setting phase to zero), or avoided, by removing the affected frequency components (by setting modulation to zero). The resulting images served as visual stimuli to determine the effects of phase errors on visual acuity for single letters, letter clusters, and faces. The results show that 180° phase reversals induced by optical aberrations reduce visual acuity, when there is sufficient contrast in the affected frequency components. In the presence of positive spherical aberration, acuity loss due to phase errors was more for hyperopic defocus than for myopic defocus, because the contrast of phase-reversed components was much higher for hyperopic defocus. Phase shifts introduced by coma are less than 180° and consequently have a smaller impact on acuity. Although visual acuity improved the most when all frequency components were phase-corrected, phase-reversed components were nevertheless found to aid visual acuity, demonstrating phase-reversed resolution.

Keywords: optical aberrations, visual acuity, phase spectrum, amplitude spectrum, face recognition, spurious resolution

Citation: Ravikumar, S., Bradley, A., & Thibos, L. (2010). Phase changes induced by optical aberrations degrade letter and face acuity. *Journal of Vision, 10*(14):18, 1–12, http://www.journalofvision.org/content/10/14/18, doi:10.1167/10.14.18.

Introduction

Most visual scenes and objects exhibit approximately 1/*f* amplitude spectra (Tadmor & Tolhurst, 1993), which led Piotrowski and Campbell (1982) to suggest that the unique appearance of an object is determined primarily by its phase spectrum. Exceptions to this conclusion arise for at least two reasons. First, although most natural targets exhibit similar global amplitude spectra, exceptions are not uncommon (Oppenheim & Lim, 1981; Srinivasan & Chandrasekaran, 1966). Second, local contrast varies significantly between targets (Field & Brady, 1997) as demonstrated by experiments in which Piotrowski and Campbell's paradigm is replicated using patch-wise Fourier analysis of the object (Morgan, Ross, & Hayes, 1991). Since the human visual system uses neural receptive fields to conduct local scene analysis (Morrone & Burr, 1988), it is likely that amplitude and phase jointly determine visual object recognition. This joint determination is complicated because visual sensitivity to phase depends on contrast (Caelli & Bevan, 1982).

The relative importance of amplitude and phase information is central to our understanding of the visual impact of optical blur due to ocular aberrations. The effect of optical defocus is to reduce retinal image contrast and alter the spatial phase relationship between frequency components (Akutsu, Bedell, & Patel, 2000; Artal, 1990; Artal, Santamaria, & Bescos, 1988; Atchison, Woods, & Bradley, 1998; Smith, 1982; Thorn & Schwartz, 1990; Walsh & Charman, 1989; Woods, Bradley, & Atchison, 1996; Zhang, Ye, Bradley, & Thibos, 1999). The visual impact of these phase changes, however, depends on the stimuli. For example, contrast sensitivity (CS; Woods et al., 1996) and visual acuity (VA; Thorn & Schwartz, 1990) for sinusoidal gratings are not affected when the spatial phase of the retinal image is reversed by optical defocus. To the contrary, when defocus reverses the phase of the high-frequency components of letters, those frequency components cease to contribute (either positively or negatively) to letter acuity (Akutsu et al., 2000; Thorn & Schwartz, 1990). This result cannot be explained by lack of visibility of the phase-reversed components because these same components can improve VA and the

doi: 10.1167/10.14.18 Received March 3, 2010; published December 15, 2010 ISSN 1534-7362

subjective appearance of broad-spectrum targets when spatial phase is corrected (Akutsu et al., 2000; Yellott & Yellott, 2007). These studies suggest that *phase-reversed resolution, defined as the ability to use phase-reversed parts of image spectra for pattern identification* (termed as "spurious resolution" by Smith, 1982, 1990; Yellott & Yellott, 2007), plays no role in defocused letter acuity.

The phase changes produced in the retinal image by optical blur depend critically upon the aberration structure of an eye (Iskander, Collins, Davis, & Carney, 2000; Sarver & Applegate, 2004). Contrast in the phase-altered portions of the defocused image spectrum varies dramatically with the sign of defocus in the presence of spherical aberration (SA; Woods et al., 1996; Zhang et al., 1999). Since most human eyes exhibit significant positive spherical aberration (Salmon & van de Pol, 2006), the visual impact of defocus-induced phase changes is likely to be greatest for hyperopic defocus. The unequal effects of positive and negative defocus on both contrast sensitivity (Guo, Atchison, & Birt, 2008; Radhakrishnan, Pardhan, Calver, & O'Leary, 2004a; Woods et al., 1996) and visual acuity (Guo et al., 2008; Radhakrishnan, Pardhan, Calver, & O'Leary, 2004b) have been linked to the underlying higher order aberrations and may reflect the different phase effects produced by positive and negative defocus. In addition, the spatial frequency range that is used to resolve or recognize a target varies with the type of target being tested. For example, face recognition employs generally lower spatial frequencies than letter recognition (compare Solomon & Pelli, 1994 with Gold, Bennett, & Sekuler, 1999). Thus, the effect of optically induced phase changes on target recognition may be target specific. It is possible to measure phase reversals in the retinal image of gratings defocused by the eye's optical system (Zhang et al., 1999). In the current experiment, our strategy was to blur the visual target so that the phase changes produced by optical blur are known and well controlled.

To assess the significance of optically induced phase changes on visual acuity, we performed a series of experiments using stimuli produced by computational optics (Akutsu et al., 2000) to answer the following questions. Are the visual effects of defocus-induced phase changes generalized to other lower and higher order aberrations? Do phase changes affect resolution for targets other than single letters? Can phase-reversed information be useful for resolution? Do the visual effects of phase changes depend on stimulus contrast?

Methods

In order to have independent control of both the amplitude and phase effects of optical aberrations, we have employed computational Fourier optics to generate blurred visual stimuli (Applegate, Ballentine, Gross, Sarver, & Sarver, 2003; Burton & Haig, 1984; Chan, Smith, & Jacobs, 1985; Cheng, Bradley, & Thibos, 2004; Legras, Chateau, & Charman, 2004). Stimuli were displayed by a high-luminance gamma-corrected digital projector viewed through a rear projection screen. MTF of the display was measured by displaying increasingly high-frequency square-wave gratings and measuring mean luminance with a photometer over a 2-pixel-wide window for gratings phase-locked to the measurement window that was alternately centered on the light and dark bars of the grating. Measured MTF of the display and the observer's diffraction-limited MTF for a 2.5-mm pupil were then deconvolved from the experimental Optical Transfer Function (OTF; Cheng, Bradley, Ravikumar, & Thibos, 2010). This ensured that retinal images were blurred only by the virtual optics in the computational model. The details of validating the equivalence of computed image and retinal image created using real lenses is documented elsewhere (Cheng et al., 2010, 2004).

The impact of optical blur on the OTF for four sample experimental conditions is shown in Figure 1. The solid lines denote the real component of the Optical Transfer Function (OTF) and dashed lines denote the angular component, the phase transfer function (PTF). A phase transition from 0 to π indicates a phase reversal and transitions in between indicate phase shifts. Adding Zernike spherical aberration (SA) typical of that encountered in human eyes (Cheng et al., 2010; Salmon & van de Pol, 2006; +0.15 μm for a 5-mm pupil) to defocus generates significant differences in the positive and negative defocus OTFs. Paraxial focus was achieved by including the required level of Z_2 to cancel the term within the Zernike spherical aberration polynomial (Cheng et al., 2010). Positive defocus in this report refers to an emmetropic eye (one that is focused paraxially) viewing a distant object through a positive spherical lens. This leaves the eye + lens system in an overpowered, myopic state. We will refer to this condition as "myopic blur." Conversely, negative defocus refers to an emmetropic eye viewing through a negative lens that is left underpowered, in a hyperopic state, which we will call "hyperopic blur." Figure 2 shows through-focus peak contrast of the first and second lobes of the OTF beyond first cutoff. Due to the dampened sine-wave form of the defocus function, the first lobe is always phase-reversed and higher in contrast than the second lobe, which is correct phase. When defocus and SA have the same sign, the phase-reversed regions of the spectrum have very low amplitudes (Figures 1B and 2). By comparison, when SA and defocus have opposite sign, the amplitudes within the phase-reversed regions of the spectrum (Figures 1A and 2) are significantly larger even when SA is an order of magnitude smaller than defocus (2.5 D is equivalent to 2.25 μm of Zernike defocus for a 5-mm pupil). This interaction between SA and defocus is also observed along the blurred meridian with cylindrical defocus

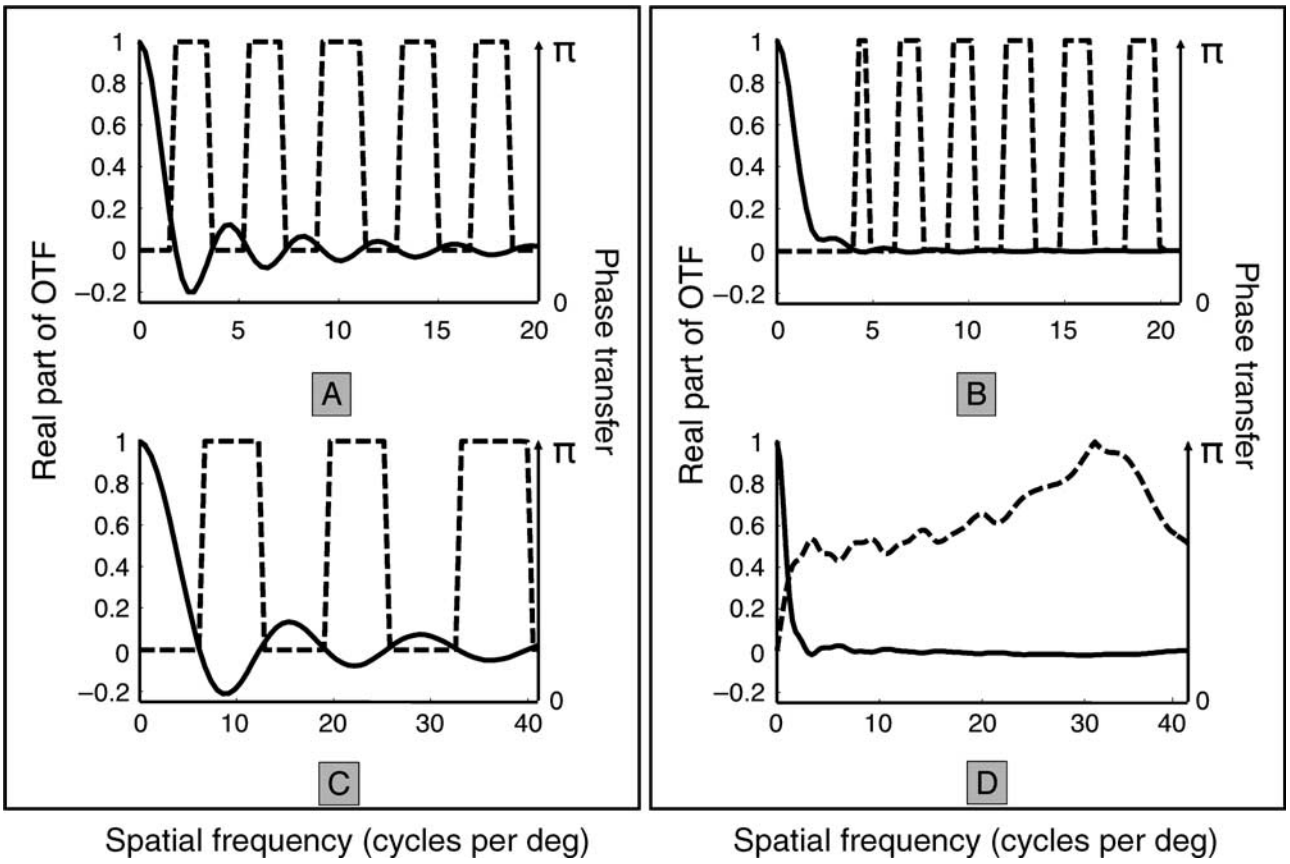

Figure 1. The real, i.e., amplitude (solid line), and angular i.e., phase (dashed line), parts of the complex-valued OTF are plotted separately for the four classes of monochromatic spatial filters (5-mm pupil) used in this study. (A) Horizontal meridian OTF for −2.5 D of (hyperopic) defocus with +0.15 μm SA. (B) Horizontal meridian OTF for +2.5 D of (myopic) defocus with +0.15 μm SA. (C) Horizontal meridian of OTF for 1DC, axis 90, and +0.15 μm of SA. (D) Vertical meridian of OTF with +1 μm of vertical coma.

(Figure 1C). Figure 1D shows the real OTF and PTF in the case of vertical coma. Only the vertical meridian OTF is plotted here. Coma introduces phase shifts that increase gradually with increasing spatial frequency, but unlike

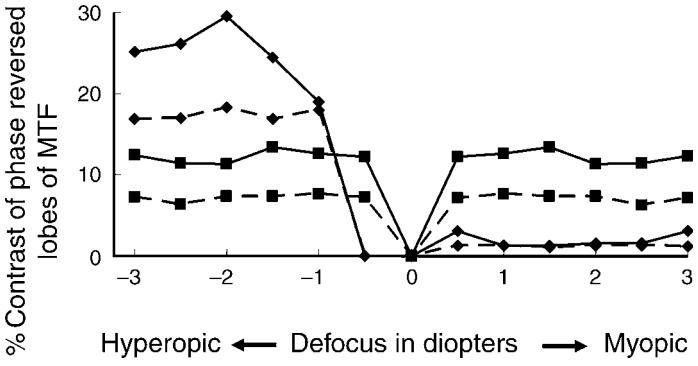

Figure 2. Peak absolute modulation transfer between first and second cutoffs (solid lines) and between second and third cutoffs (dashed lines) of the MTF is plotted as a function of spherical defocus in the presence and absence of positive spherical aberration (diamonds and squares, respectively). Contrast has been normalized to the diffraction-limited maximum.

spherical and cylindrical defocus, the phase changes are not restricted to π phase reversals.

Displaying images that have been blurred computationally poses some interesting challenges for image rendering. First, the deconvolution process (Burton & Haig, 1984; Peli & Lang, 2001) requires that images with amplified high-frequency content be computed and displayed. Thus, 100% contrast letter targets will require computed images to exceed the 8-bit resolution limit of the system (Cheng et al., 2010). This problem is resolved by reducing the pre-filtered target contrast to 21%.

We tested visual acuity for experimental stimuli that were blurred with different types of filters (Figure 3). We investigated the impact of blur-induced phase changes by comparing the impact of normal blur filter (which includes both demodulation and phase changes, Figure 3A) to blur produced only with demodulation. Demodulation only blur was generated by setting the PTF to zero (phase-corrected case, Figure 3B) or simply by eliminating all modulation above first zero of the OTF (low-pass filter case, Figure 3C; Akutsu et al., 2000; Yellott & Yellott, 2007).

If vision with the phase-corrected filter (Figure 3B) is better than the normal filter (Figure 3A), it indicates that

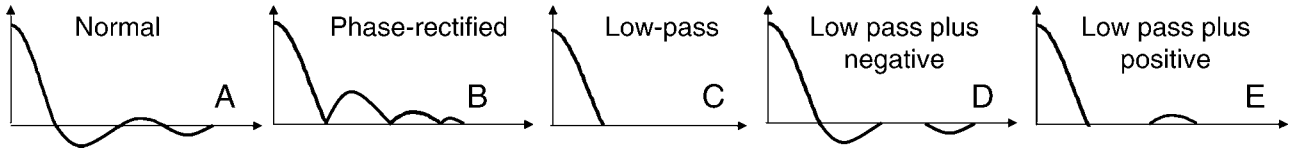

Figure 3. Schematic of the real part of the complex-valued optical transfer function as a function of spatial frequency.

phase changes reduce visual acuity. If vision with the normal optical filter produced better VA than with a low-pass filter (Figures 3A and 3C, respectively), it raises the question of whether a potential loss in VA with the low-pass filter is due to the loss of phase-reversed or phase-correct lobes of the OTF beyond the first OTF zero. One possible hypothesis is that it is the frequencies in veridical phase beyond the first cutoff that aid VA. Alternately, one can hypothesize that phase-reversed lobes of the defocused image spectrum of the defocused OTF retain some value and contribute to VA, because of phase-reversed resolution. A third possibility is that the correct phase sections of the phase alternating region of the OTF may aid VA and the reverse phase sections interfere with VA. In order to test these hypotheses, we further investigated VA using two additional filters (Figures 3D and 3E). A low-pass plus negative lobe filter (Figure 3D) was used to test whether the phase-reversed portions of the spectrum contribute to visual resolution. A low-pass plus positive lobe filter (Figure 3E) was used to test whether small amounts of correct phase signal beyond the second cutoff contribute to resolution. Although the low-pass plus negative as well as low-pass plus positive filters (Figures 3D and 3E, respectively) generate point-spread functions (PSF) with negative lobes, they produce strictly positive images of 21% contrast targets.

Three different VA tasks were examined: single letters (Sloan letter set, 1 of 10 identification tasks), 3 × 3 clusters of Sloan letters (the task was to identify the central letter alone, 1 of 10 identifications), and facial expression identification (10 different people with happy or sad expressions (Zhang & Cottrell, 2004), 1 of 2 identifications). For the clustered letter condition, all 9 letters were equal in size and separation between the letters was equal to 1 stroke width. Previous studies have shown that a letter separation of up to 1.2 stroke widths is sufficient to cause crowding for foveal viewing of focused targets (Chung, Levi, & Legge, 2001; Leat, Li, & Epp, 1999). When defocused, letters on the margin span the gap between letters and partially overlap the central letter that is to be identified. This stimulus configuration is more challenging than single letters and is intended to represent the common task of reading text. The face stimuli were provided courtesy of Dr. Cottrell (Zhang & Cottrell, 2004). Since the face stimuli lack sharp contours, we were able to run the psychophysical experiment at a higher contrast of 44% while still being able to correct for the display and subject's optics.

The method of constant stimuli was used for the psychophysical experiment. Approximately 100 black-on-white stimuli (10 stimuli at 10 sizes) were used to capture an entire psychometric function. Stimuli were presented one at a time for 0.5 s, signaled by a tone. Both the letter and its size were chosen at random, while ensuring that every letter from the Sloan set was displayed at least once at each size. All the faces, in entirety, were also displayed at least once at each size (see example in Figure 5C). For every presentation, the letter chosen by the algorithm was Fourier transformed to obtain its amplitude and phase spectrum, which was then multiplied by the OTF of the desired filter. All the OTFs had a constant digital size of 512 * 512. Therefore, the letter of choice at each presentation was padded to 512 * 512 pixels before being Fourier transformed. The filtered letter was then inverse Fourier transformed to obtain the blurred image for display. This procedure ensures that the spatial frequency spectrum of the letter scales within the optical bandwidth of the filter.

The response matrix of the subject was used to estimate proportion correct at each size. Raw performance data were fit with a Weibull function using least squares regression (Cheng et al., 2010). Criterion for threshold performance was set halfway between chance (10% for 1 of 10 identifications and 50% for 1 of 2 identifications) and 100% performance. VA is reported as the letter size at criterion performance in log MAR units. Estimated coefficient parameters were then used to estimate the 95% confidence interval of VA. Half of the total interval between best and worst VA estimates was considered to be the confidence interval half-width. VA was considered to be statistically significantly different if the 95% confidence interval of the estimates did not overlap. All programming necessary for computational implementation of the blur and filters was done using MATLAB (Mathworks, MA). The psychophysics programs were written with the help of psychtoolbox (Brainard, 1997).

Subjects viewed test stimuli monocularly through a unit magnification telescope that imaged an artificial aperture of 2.5-mm diameter into the plane of the observer's entrance pupil (Cheng et al., 2010). The rear projection screen that displayed the stimuli was placed 2.48 m from the artificial pupil. Screen edges were well focused and high contrast. Result figures show data from a presbyopic subject and the main results were confirmed on a younger second subject. The two subjects were

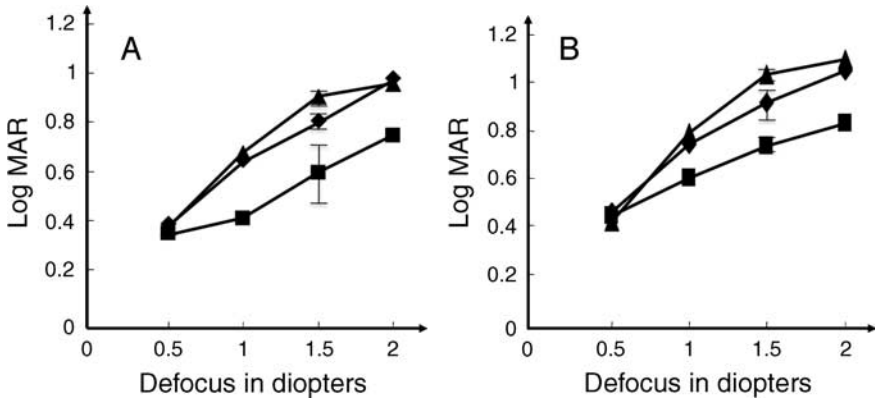

Figure 4. Visual acuity as a function of spherical defocus with three different filters, normal defocus (diamonds), phase-rectified (squares), and low-pass (triangles). (A) Results for single letter stimuli. (B) Results with a 3 * 3 cluster of letters. Error bars denoting 95% confidence interval are shown for representative data at 1.5-D defocus in both (A) and (B), for all three filters.

fully corrected for distance vision with their prescription. The display was monochromatic at 550 nm and had a luminance of 225 cd/m^2.

Results

Effect of spherical defocus

Using images blurred by spherical defocus only, we confirmed an earlier report (Akutsu et al., 2000) showing that removing the spectrum above the first cutoff (our Low-pass condition, Figure 3C) has little or no effect on defocused VA (Figure 4A). This indicates that, in most cases, VA for single letters blurred only by spherical defocus is determined by that part of the image spectrum below the first cutoff. With 1.5 D of defocus, we observed a small (<0.1 log MAR) but significant increase in log MAR when removing the spatial frequencies above the first cutoff. This result, generalized to more complex stimuli (3 × 3 letter arrays, Figure 4B), confirms that phase-reversed resolution does not occur for letter targets blurred by spherical defocus alone. For both stimulus configurations, rectifying phase improved log MAR VA relative to normal defocus filter by approximately 0.2, for defocus levels of 1.0 to 2.0 diopters (vertical black bars denote 95% confidence interval of VA measurement in all result figures), showing that the spectrum above the first cutoff has sufficient contrast to be visually useful when phase corrected but insufficient to produce normal focused VA. Since the improvement occurs only when phase is rectified, the resolution is not "phase-reversed" in the sense defined in the Introduction section. These results demonstrate that the reduction in VA due to spherical defocus can be attributed in part to contrast reduction and partly to the accompanying phase reversals (VA was significantly better, but not 20/20 after phase correction).

When defocus is combined with positive spherical aberration, the visual impact of phase correction depended on the sign of defocus (Figure 5). Best VA was observed with 0.5 D of defocus (relative to paraxial focus) consistent with previous reports from our laboratory (Cheng et al., 2010, 2004). With induced myopic defocus (positive defocus), VA remained the same with all three types of filters (normal, phase-rectified, and low-pass). This result is consistent across all three stimuli types (Figures 5A–5C) and for both observers, confirming the expectation based on Figure 1 that myopic defocus degrades VA because of the OTF demodulation and not because of the accompanying phase changes. The differences in acuity between the three filters tested were statistically significant only for induced hyperopic defocus greater than 1 D (Figure 5A). VA with a second subject was measured with 2 D and +2 D for all three filters and the results are consistent with that of the first subject. For the second subject, VAs, in log MAR units with +2 D, were 0.71 (both normal and low-pass filters) and 0.72 (phase-rectified filter). VAs with 2-D defocus were 0.37 (normal filter), 0.17 (phase-rectified filter), and 0.47 (low-pass filter). That is, with induced hyperopic defocus, the defocus-induced degradation in VA is exaggerated by low-pass filtering but improved with phase correction. Qualitatively similar results were found for a range of defocus levels as shown in Figure 6. For example, with 2.5-D defocus, phase correction increased VA by almost 0.4 log MAR, whereas low-pass filtering reduced VA by about 0.3 log MAR.

Presence of phase-reversed resolution

To determine which frequencies beyond the first cutoff contribute to VA, testing was done with two additional filters, low-pass plus negative and low-pass plus positive (Figures 3D and 3E). Single letter VA was tested with 2.5

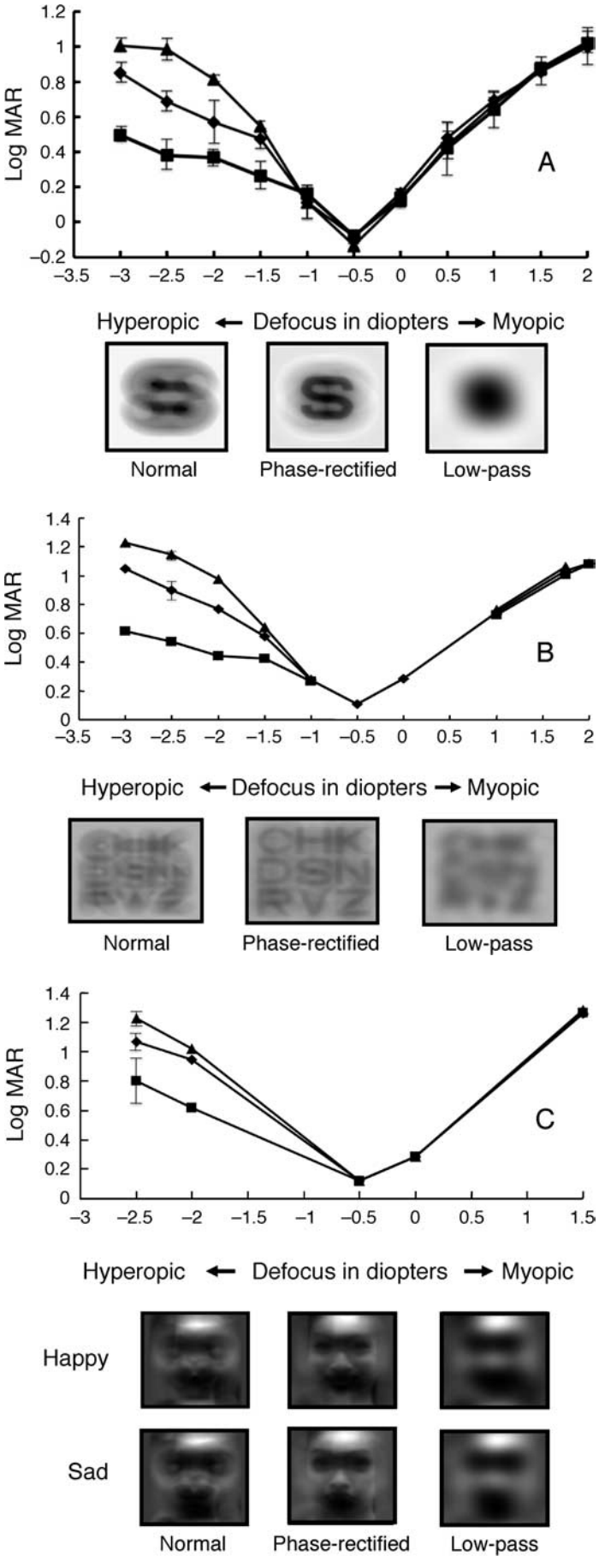

Figure 5. Through-focus visual acuity in the presence of 0.15 μm (0.17 equivalent diopters) of spherical aberration, for three filters, normal defocus (diamonds), phase-rectified (squares), and low-pass (triangles). Visual acuity results for single letters are shown in (A), clusters of letters in (B), and face stimuli in (C). Sample images of test stimuli all blurred by −2.5 D are shown in each panel; size of the images in angular units: (A) 22.5 arcmin; (B) 40 arcmin; and (C) a 1-degree face. These sizes were chosen to be close to threshold for the normal filter case, to show the relative improvement due to phase rectification as well as the loss in image quality with low-pass filtering.

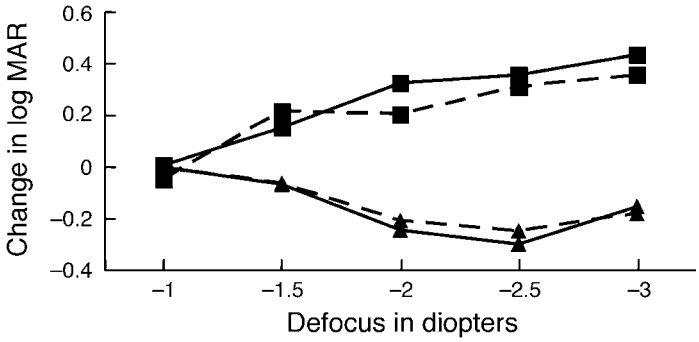

Figure 6. Change in log MAR VA from the normal defocus test condition as a function of defocus level with 2 different filters and stimuli. Gain is quantified as positive and loss as negative. Solid lines represent data for single letters and dashed lines for letter clusters; squares represent data with phase-rectifying filter; and triangles represent data for low-pass filter.

diopters of hyperopic (negative) defocus with 0.15 μm of positive SA and repeated 5 times for each filter with 21% stimulus contrast (Figure 7). The differences in VA for normal, phase-rectified, and low-pass filters are consistent with results in Figure 5A. Pairwise *t*-tests were conducted for the different conditions. Acuity with low-pass plus negative and low-pass plus positive filters was better than for low-pass filter (p = 0.00086 for filters C and D comparison and p = 0.000843 for filters C and E comparison) and similar to that observed with the normal defocus filter. Acuity with low-pass plus positive filter was slightly worse than for low-pass plus negative filter (p = 0.044, mean difference = 0.08 log MAR), indicating that signal amplitudes within the negative contrast lobes were slightly better at improving VA than those within the positive contrast lobes. This superiority of VA for low pass plus negative compared to low pass is evidence for "phase-reversed resolution." The fact that VA for low-pass plus negative filter was significantly worse than for the phase-rectified filter (p = 0.00023) but significantly better than low-pass filter affirms that, although the frequency components with non-veridical phase are more useful than no information, they are not as beneficial as when they are in the right phase.

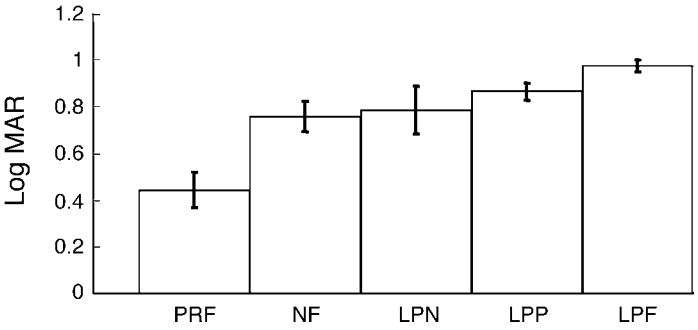

Figure 7. Single letter VA for 5 different filters with −2.5-D defocus and +0.15 μm of SA. The legend from left to right: NF—normal filter; PRF—phase-rectified filter; LPF—low-pass filter; LPN—low-pass plus negative; LPP—low-pass plus positive. Error bars (±2 *SE*) are in black. Filter letters follow Figure 3 notation.

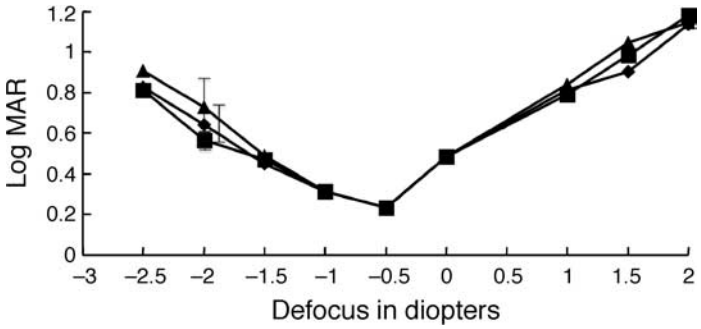

Figure 8. Low contrast (4%) VA in one subject with 0.15 μm of positive SA. Triangles, diamonds, and squares, respectively, denote low-pass, normal, and phase-rectified filters; 95% confidence intervals are shown for −2-D VA data. Error bar for normal filter data has been laterally displaced for clarity.

Effect of contrast

We have observed phase-reversed resolution under conditions (positive SA, hyperopic defocus) where the amplitude of phase-reversed section of the defocused OTF is about 25–30% and failed to observe it under conditions where the phase-reversed portions of the defocused spectrum has lower contrast (12.24% for defocus alone and ~2% for positive SA and myopic defocus). This result is consistent with the notion that myopic blur and SA in combination fail to generate phase-reversed resolution because there is insufficient contrast in the phase-reversed sections of the image spectrum to improve visual performance. By extension, we can hypothesize that if the stimulus contrast were low enough, then phase rectification would not be useful even in the case of hyperopic defocus and SA.

To test this contrast dependence hypothesis for phase-reversed resolution, we repeated the through-focus plus SA experiment with low-contrast (4%) single letters. Contrary to the high-contrast hyperopic defocus results, the low-contrast VAs showed virtually no effect of phase manipulation (Figure 8). VA differences at 2.5 D of defocus, between the three filters (normal, phase-rectified, and low-pass), were found to be statistically insignificant. This result indicates that the phase-reversed resolution shown in Figure 7 is restricted to higher contrast targets. Even when phase is corrected, the higher frequency content in the image spectrum had insufficient contrast to aid VA for low-contrast targets.

Effect of phase changes created by meridionally varying aberrations

The results of phase manipulation thus far have been shown for aberrations that are circularly symmetric. However, the phase errors in non-symmetric aberrations will vary with meridian. We examined the impact of meridian-specific phase manipulations for the case of cylindrical defocus (axis 90 astigmatism) in combination with positive SA. The results (Figure 9) are similar to those observed with spherical defocus (Figure 5A), indicating that, as with spherical defocus, VA loss with cylindrical defocus of the opposite sign to the SA is due in part to phase changes and in part due to demodulation.

In all the above aberrations, the phase errors caused by optical aberrations are 180-degree phase reversals. However, optically induced phase errors can also vary gradually across the spatial frequency spectrum such as those produced by coma (Figure 1D). Since coma does not cause complete phase reversals, there is no distinct cutoff.

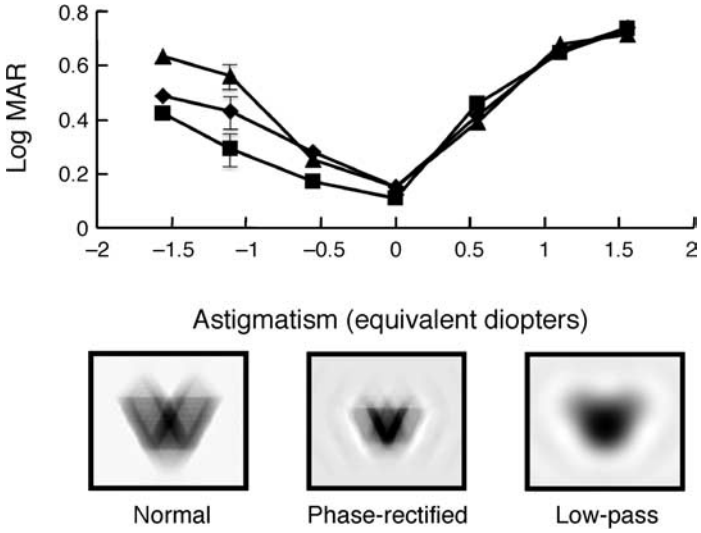

Figure 9. Visual acuity with axis 90 cylindrical defocus and Seidel SA for the normal, phase-rectified, and low-pass filters (diamonds, squares, and triangles, respectively). The sample images of the letter V (12.5 arcmin) are representative of the type of stimuli seen with the three filters with 1.1 D of cylindrical defocus; 95% confidence interval for VA data, at −1.1 D of astigmatism, has been shown.

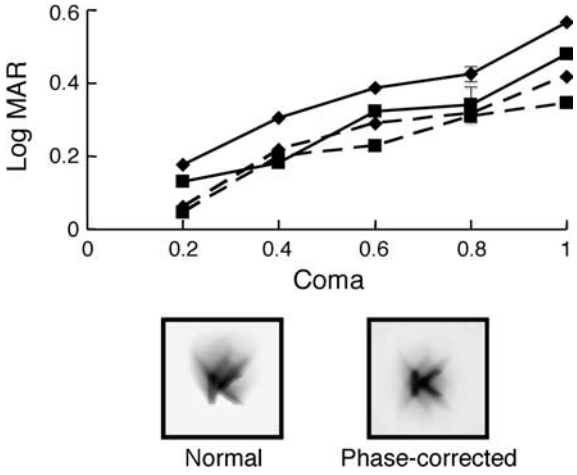

Figure 10. VA is plotted as a function of coma (micron rms of wavefront error). Dashed lines represent single letter stimuli and continuous lines represent data for cluster of letters. Data with the normal coma filter are plotted with diamonds and phase-corrected filter with squares. Sample images are shown for a 25-arcmin letter with 1-μm coma; 95% confidence interval estimates for the cluster paradigm are shown, at 0.8 μm of coma.

Therefore, in this experiment, we only compare the normal blur caused by coma to the phase-corrected case. The single letter and letter cluster VA data for coma are shown in Figure 10. Similar to the other results so far, VA with single letters is slightly better (mean difference of 0.11 log unit) than with a cluster of letters. The improvement in VA produced by phase correction is larger for the letter cluster stimuli across a wide range of coma (0.4 to 1.0 μm). Mean improvement with phase correction was 0.03 log unit with single letters and 0.08 log unit with cluster stimuli.

Discussion

Consistent with the predictions of Walsh and Charman (1989) and the observations of Yellott and Yellott (2007) and Akutsu et al. (2000), our experiments show (Figures 4–10) that correcting the phase changes introduced by optical aberrations can improve VA. We also show that this is true for a range of optical aberration types and levels and for different stimuli. However, we show that this effect is not universal and is absent when the phase-altered regions of the defocused image spectra have low contrast due to either low object contrast or low modulation transfer in the phase-altered regions of the OTF. Our experiments comparing normal defocus to the low-pass filter case (Figure 5) and the low-pass plus negative filter (Figure 7) emphasize that the phase-reversed regions of the defocus spectra can aid in resolving fine detail of broad spectrum stimuli. That is, we confirm the utility of phase-reversed resolution in letter recognition, contrary to previous reports (Akutsu et al., 2000; Thorn & Schwartz, 1990). In addition, we show that improvement with phase correction is also seen when the stimuli are a cluster of letters or a set of faces. This shows that phase changes associated with optical aberrations are likely to impair performance in common tasks of reading and face recognition.

Most striking is the finding that myopic defocus causes reduced VA because of decreased image modulation, whereas hyperopic defocus reduces VA because of both amplitude demodulation and phase changes (Figure 5). These differences in the origin of myopic and hyperopic vision losses may explain the observations of unequal effects of positive and negative defocus on vision (Guo et al., 2008; Radhakrishnan et al., 2004a, 2004b; Vasudevan et al., 2010; Woods et al., 1996). Thus, hyperopes and presbyopes viewing near targets with positive SA, unlike myopes viewing distant targets with positive SA, would benefit from a phase-corrected image. The fact that phase correction does not eliminate the effect of defocus shows that the visual impact of defocus is due in part to amplitude demodulation as well as phase reversals even in the case of hyperopic defocus with positive SA. Comparing the normal defocus with the phase-corrected defocus data in Figures 5A and 5B indicates that, for hyperopes and presbyopes, demodulation contributes to about 60% of the loss of log MAR VA. It is clear from these studies that, as suggested by Sarver and Applegate (2004), measures of optical quality in human eyes should not be restricted to modulation metrics based on the MTF. A better metric would be one that not only weights the modulation information by the contrast sensitivity function but provides separate additional independent weighting for bands that are phase-reversed compared to those that are phase correct. The importance of frequencies beyond first cutoff is demonstrated by the accuracy of metrics like VSOTF in predicting subjective visual quality (Cheng et al., 2004).

Although our experiments highlight the significance of phase changes introduced by optical defocus, it is important to note that the impact of phase tended to increase with the level of defocus, and for low levels of defocus and low levels of coma, we observed no effect of phase correction. This is mainly because phase reversals were not generated by low defocus (first π phase shift is seen at about 0.5 D for a 5-mm pupil diameter; Walsh & Charman, 1989).

The importance of defocus-induced phase changes in determining VA for hyperopes and presbyopes raises the important question of whether the phase changes influence VA by changing the global structure of the image (as demonstrated by Piotrowski and Campbell, 1982) or by disrupting the local phase alignment required to generate contrast in spectrally broadband targets (Morrone & Burr, 1988). Several of the sample images shown in the Results section confirm that defocus-induced phase changes can generate very noticeable changes in image structure (e.g., Figures 5 and 9). For example, negative cylindrical

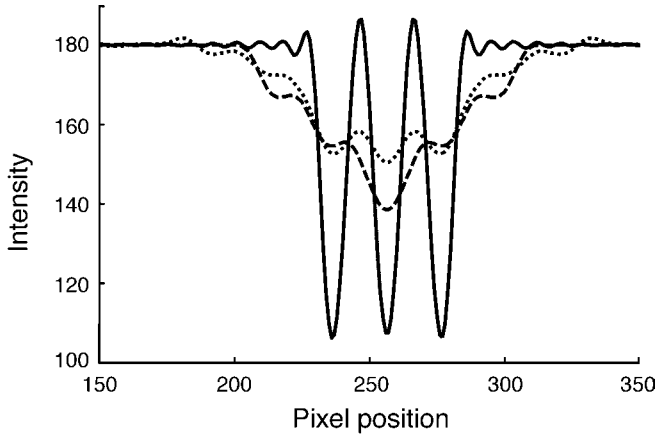

Figure 11. Intensity profile across a 20/50 letter E, with −1.5 D of hyperopic defocus and +0.15 μm spherical aberration. Three filter conditions are shown: diffraction-limited (solid line), normal defocus (dashed line), phase-corrected (dotted line).

defocus in combination with positive SA caused the images to appear diplopic along the horizontal axis or "ghosted," with the letter V appearing similar to letter "W." In addition, spherical defocus and spherical aberration seemed to change solid letters into outlines (e.g., see letter S in Figure 5A). Optically induced structural changes, e.g., diplopia and contour sign reversal, have been reported previously (Woods et al., 1996; Yellott & Yellott, 2007). However, as predicted by Morrone and Burr (1988), the phase-corrected images in Figure 5 exhibit higher contrast than images created with normal defocus.

We have employed three quantitative approaches to assess the impact of optically induced phase changes on image structure and image contrast. Global image contrast was assessed by computing the standard deviation of the image intensities (rms contrast measure; Peli, 1990, Equation 4a). This analysis revealed, as expected, that the blurred image and the phase-corrected images have identical overall rms contrast. Therefore, contrast per se cannot explain the difference in VA measured with these two filters. A second analysis showed that local contrast at the border of blurred letters was dramatically increased by phase correction. For example, the intensity profile across an image of a defocused letter E of size 12.5 arcmin (Figure 11) shows that phase correction increases image contrast and alters the position of the border contrasts to better match the focused diffraction-limited template. In the examples shown in Figure 11, defocus has reduced the contrast of the outer edges in the defocused E and reversed the contrast of the inner edges, essentially replacing 3 parallel letter strokes with a single dark bar. Phase correction reestablishes contrast throughout the extent of the image, albeit not to the level of a diffraction-limited system. Contrast across these "edges" was quantified by calculating the slope along the vertical meridian for a rightward facing letter "E." As predicted by Morrone and Burr (1988), phase correction increased slope of these edges by returning the phase synchronization that characterizes an edge.

The impact of phase on image structure can be assessed independent of global contrast by comparing the cross-correlations of the blurred, focused, and phase-corrected images. Normalized correlation coefficients (Lewis, 1995, Equation 2) shown here in Equation 1 were calculated for image pairs of letter "E" (rightward facing) with a 5-mm pupil, 20/90 size letter. Dioptric blur was varied with spherical aberration, just as in Figure 5. The correlation coefficient results are shown in Table 1:

$$\gamma(u,v) = \frac{\sum_{x,y}[f(x,y) - \bar{f}_{u,v}][t(x-u,y-v) - \bar{t}]}{\sqrt{\sum_{x,y}[f(x,y) - \bar{f}_{u,v}]^2 \sum_{x,y}[t(x-u,y-v-\bar{t})]^2}} \quad (1)$$

In the above equation, $\gamma(u, v)$ is the normalized cross-correlation coefficient between two images, is the mean of the feature $f_{u,v}$ and is the mean of $f(x, y)$ in the region

	Cross-correlation coefficient			VA data (log MAR)	
Blur level	Diffraction-limited template vs. blurred image	Template vs. phase-rectified image	Blurred vs. phase-rectified image	Phase-rectified filter	Normal filter
−2.5	0.44	0.66	0.89	0.54	0.89
−1.5	0.72	0.79	0.98	0.42	0.58
−0.5	0.95	0.95	1	0.11	0.11
0.5	0.73	0.73	1	0.52	0.52
1.5	0.55	0.55	0.99	0.88	0.92

Table 1. Cross-correlation between different images used in the psychophysical study. All correlations have been calculated for images that in addition to the blur levels in diopters indicated in the leftmost column also had +0.15 μm of spherical aberration. Images of 20/90 letters were used for the analysis. Data are shown under the columns titled "Cross-correlation coefficient." VA data for the normal and phase-rectified filter for corresponding blur levels are shown in the rightmost 2 columns. *Note*: VA data on the myopic side for 0.5 D are a linear interpolate from measured values at 0 D and +1 D and at +1.5 D are a linear interpolate between measured values at +1 and +1.75 D.

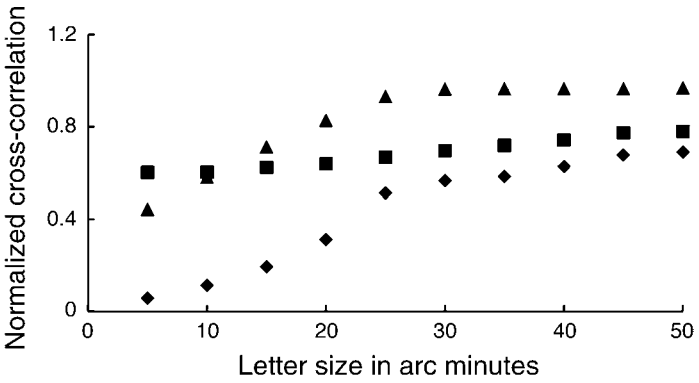

Figure 12. Cross-correlation as a function of letter size between the diffraction-limited image template and the defocused image (diamonds), diffraction-limited template and phase-corrected images (squares), and the cross-correlation between the blurred and the phase-corrected letters (triangles). These cross-correlations were computed for a 5-mm pupil with +0.15 μm of SA and −2.5 D of spherical defocus.

under the feature. The maximum value of this function is taken to be the correlation coefficient.

From Table 1 correlation values, it can be seen (columns 2 and 3) that phase correction improves cross-correlation with the diffraction-limited template for all blur levels except for low levels of blur (+0.5 and −0.5 D). The improvement in correlation is far greater for the negative defocus and increases with increase in blur. This can also be seen reflected in the correlation values (Table 1, column 4) of the normal defocus and the phase-corrected image. With highest blur level, 2.5 D, these two images are not correlated well, which reiterates structural changes introduced by the phase changes independent of the amplitude demodulation, which is common to both.

We have extended the above cross-correlation analysis to evaluate the impact of letter size on the ability of defocus to alter structure of the image (Figure 12). For a given aberration level (+0.15 μm of SA and 2.5 D of defocus), we find that cross-correlation between the focused template image and the normal blurred version of the letter drops as letter size decreases and approaches zero for 20/20 letters (angular size 5 arcmin). However with phase correction, even the smallest 20/20 letter maintains a 0.6 correlation value. Correlation between the normal blur and phase-corrected blur remains close to 1 for a 20/100 (angular size 25 arcmin) or larger letter but drops to 0.4 for 20/20 letters. These results emphasize that for larger targets, the impact of blur is primarily one in which local edge contrast is demodulated, but for smaller characters, the phase changes begin to disrupt the global structure of the image and thus blurred and phase-corrected images are no longer highly correlated. The close relationship between cross-correlation analysis and psychophysical behavior of the subject suggests that an improvement in image fidelity due to phase rectification has contributed to a task-based improvement in image quality for letter recognition.

Although we have examined the impact of optically induced phase changes on VA, there are studies indicating that the human visual system is phase blind for very high spatial frequencies (Kulikowski, 1978) or unable to employ phase information at very high spatial frequencies because of low-contrast and high-contrast thresholds (Bradley & Skottun, 1987; Caelli & Bevan, 1982). In spite of these reports, humans can reliably identify 20/13 letters (3.25 arcmin; Elliot, Yang, & David Whitaker, 1995) indicating that the phase structure beyond 30 c/deg can be resolved with sufficient accuracy to discriminate letters. The importance of defocus-induced phase changes indicate that, in order to adapt to optical defocus, the neural system must be able to adapt to both amplitude and phase changes, as suggested by studies of adaptation to spherical and astigmatic defocus (Mon-Williams, Tresilian, Strang, Kochhar, & Wann, 1998; Ohlendorf & Schaeffel, 2009; Pesudovs & Brennan, 1993; Rosenfield, Hong, & George, 2004; Sawides et al., 2010).

Acknowledgments

This research was supported in part by National Institutes of Health Grant NEI RO1 EY05109 (L.N.T).

Commercial relationships: none.
Corresponding author: Sowmya Ravikumar.
Email: ravikumar@berkeley.edu.
Address: 360 Minor Hall, University of California Berkeley, CA, USA.

References

Akutsu, H., Bedell, H. E., & Patel, S. S. (2000). Recognition thresholds for letters with simulated dioptric blur. *Optometry and Vision Science, 77,* 524–530. [PubMed] [Article]

Applegate, R., Ballentine, C., Gross, H., Sarver, E., & Sarver, C. (2003). Visual acuity as a function of Zernike mode and level of root mean square error. *Optometry and Vision Science, 80,* 97–105. [PubMed] [Article]

Artal, P. (1990). Calculations of two-dimensional foveal retinal images in real eyes. *Journal of the Optical Society of America A, 7,* 1374–1381. [PubMed] [Article]

Artal, P., Santamaria, J., & Bescos, J. (1988). Phase-transfer function of the human eye and its influence on point-spread function and wave aberration. *Journal*

of the Optical Society of America A, 5, 1791–1795. [PubMed] [Article]

Atchison, D., Woods, R., & Bradley, A. (1998). Predicting the effects of optical defocus on human contrast sensitivity. *Journal of the Optical Society of America A, 15,* 2449–2456. [PubMed] [Article]

Bradley, A., & Skottun, B. (1987). Effects of contrast and spatial frequency on vernier acuity. *Vision Research, 27,* 1817–1824. [PubMed] [Article]

Brainard, D. H. (1997). The psychophysics toolbox. *Spatial Vision, 10,* 433–436. [PubMed] [Article]

Burton, G., & Haig, N. (1984). Effects of the Seidel aberrations on visual target discrimination. *Journal of the Optical Society of America A, 1,* 373–385. [PubMed] [Article]

Caelli, T., & Bevan, P. (1982). Visual sensitivity to two-dimensional spatial phase. *Journal of the Optical Society of America, 72,* 1375–1381. [PubMed] [Article]

Chan, C., Smith, G., & Jacobs, R. J. (1985). Simulating refractive errors: Source and observer methods. *American Journal of Physiological Optics, 62,* 207–216. [PubMed]

Cheng, X., Bradley, A., Ravikumar, S., & Thibos, L. N. (2010). A comparison of the effects of Siedel and Zernike aberrations on visual acuity for monochromatic light. *Optometry and Vision Science, 27,* 300–312. [PubMed] [Article]

Cheng, X., Bradley, A., & Thibos, L. N. (2004). Predicting subjective judgment of best focus with objective image quality metrics. *Journal of Vision, 4*(4):7, 310–321, http://www.journalofvision.org/content/4/4/7, doi:10.1167/4.4.7. [PubMed] [Article]

Chung, S. T. L., Levi, D. M., & Legge, G. E. (2001). Spatial frequency properties and contrast properties of crowding. *Vision Research, 41,* 1833–1850. [PubMed] [Article]

Elliot, D. B., Yang, K. C. H., & David Whitaker, P. D. (1995). Visual acuity changes throughout adulthood in normal, healthy eyes: Seeing beyond 6/6. *Optometry and Vision Science, 72,* 186. [PubMed] [Article]

Field, D. J., & Brady, N. (1997). Visual sensitivity, blur and the sources of variability in the amplitude spectra of natural scenes. *Vision Research, 37,* 3367–3383. [PubMed] [Article]

Gold, J. M., Bennett, P. J., & Sekuler, A. B. (1999). Identification of band-pass filtered letters and faces by human and ideal observers. *Vision Research, 39,* 3537–3560. [PubMed] [Article]

Guo, H., Atchison, D. A., & Birt, B. J. (2008). Changes in through-focus spatial visual performance with adaptive optics correction of monochromatic aberrations. *Vision Research, 48,* 1804–1811. [PubMed] [Article]

Iskander, D., Collins, M., Davis, B., & Carney, L. (2000). Monochromatic aberrations and characteristics of retinal image quality. *Clinical and Experimental Optometry, 83,* 315–322. [PubMed] [Article]

Kulikowski, J. J. (1978). Spatial resolution for the detection of pattern and movement (real and apparent). *Vision Research, 18,* 237. [PubMed] [Article]

Leat, S. J., Li, W., & Epp, K. (1999). Crowding in central and eccentric vision: The effects of contour interaction and attention. *Investigative Ophthalmology and Visual Science, 40,* 504–512. [PubMed] [Article]

Legras, R., Chateau, N., & Charman, W. (2004). Assessment of just-noticeable differences for refractive errors and spherical aberration using visual simulation. *Optometry and Vision Science, 81,* 718–728. [PubMed] [Article]

Lewis, J. P. (1995). *Fast Template Matching*. Paper presented at Vision Interface 95, Canadian Image Processing and Pattern Recognition Society, Quebec City, Canada, May 15–19, p. 120–123. [Article]

Mon-Williams, M., Tresilian, J. R., Strang, N. C., Kochhar, P., & Wann, J. P. (1998). Improving vision: Neural compensation for optical defocus. *Proceedings of Biological Sciences, 265,* 71–77. [PubMed] [Article]

Morgan, M. J., Ross, J., & Hayes, A. (1991). The relative importance of local phase and local amplitude in patch-wise image reconstruction. *Biological Cybernetics, 65,* 113–119. [Article]

Morrone, M. C., & Burr, D. C. (1988). Feature detection in human vision: A phase-dependent energy model. *Proceedings of the Royal Society of London B: Biological Sciences, 235,* 221–245. [PubMed] [Article]

Ohlendorf, A., & Schaeffel, F. (2009). Contrast adaptation induced by defocus—A possible error signal for emmetropization? *Vision Research, 49,* 249–256. [PubMed] [Article]

Oppenheim, A., & Lim, J. (1981). The importance of phase in signals. *Proceedings of the IEEE, 69,* 529–541. [Article]

Peli, E. (1990). Contrast in complex images. *Journal of the Optical Society of America A, 7,* 2032–2040. [PubMed] [Article]

Peli, E., & Lang, A. (2001). Appearance of images through a multifocal intraocular lens. *Journal of the Optical Society of America A, 18,* 302–309. [PubMed] [Article]

Pesudovs, K., & Brennan, N. A. (1993). Decreased vision after a period of distance fixation with spectacle wear. *Optometry and Vision Science, 70,* 528–531. [PubMed] [Article]

Piotrowski, L. N., & Campbell, F. W. (1982). A demonstration of the visual importance and flexibility of spatial-frequency amplitude and phase. *Perception, 11,* 337–346. [PubMed] [Article]

Radhakrishnan, H., Pardhan, S., Calver, R. I., & O'Leary, D. J. (2004a). Effect of positive and negative defocus on contrast sensitivity in myopes and non-myopes. *Vision Research, 44,* 1869–1878. [PubMed] [Article]

Radhakrishnan, H., Pardhan, S., Calver, R. I., & O'Leary, D. J. (2004b). Unequal reduction in visual acuity with positive and negative defocusing lenses in myopes. *Optometry and Vision Science, 81,* 14–17. [PubMed] [Article]

Rosenfield, M., Hong, S. E., & George, S. (2004). Blur adaptation in myopes. *Optometry and Vision Science, 81,* 657–662. [PubMed] [Article]

Salmon, T. O., & van de Pol, C. (2006). Normal-eye Zernike coefficients and root-mean-square wavefront errors. *Journal of Cataract and Refract Surgery, 32,* 2064–2074. [PubMed] [Article]

Sarver, E. J., & Applegate, R. A. (2004). The importance of the phase transfer function to visual function and visual quality metrics. *Journal of Refractive Surgery, 20,* S504–S507. [PubMed] [Article]

Sawides, L., Marcos, S., Ravikumar, S., Thibos, L. N., Bradley, A., & Webster, M. A. (2010). Adaptation to astigmatic blur. *Journal of Vision, 10*(12):22, 1–15, http://www.journalofvision.org/content/10/12/22, doi:10.1167/10.12.22. [PubMed] [Article]

Smith, G. (1982). Ocular defocus, spurious resolution and contrast reversal. *Ophthalmic and Physiological Optics, 2,* 5–23. [PubMed] [Article]

Smith, W. J. (1990). *Modern optical engineering* (2nd ed.). New York: McGraw-Hill.

Solomon, J. A., & Pelli, D. G. (1994). The visual filter mediating letter identification. *Nature, 369,* 395–397. [PubMed] [Article]

Srinivasan, R., & Chandrasekaran, R. (1966). Correlation functions connected with structure factors and their application to observed and calculated structure factors. *Indian Journal of Pure and Applied Physics, 4,* 178–186.

Tadmor, Y., & Tolhurst, D. J. (1993). Both the phase and the amplitude spectrum may determine the appearance of natural images. *Vision Research, 33,* 141–145. [PubMed] [Article]

Thorn, F., & Schwartz, F. (1990). Effects of dioptric blur on Snellen and grating acuity. *Optometry and Vision Science, 67,* 3–7. [PubMed] [Article]

Vasudevan, B., Bradley, A., Thibos, L. N., Martin, J., Nam, J., & Himebaugh, N. L. (2010). Impact of positive and negative defocus on visual acuity. *Investigative Ophthalmology and Vision Science, 51,* E-Abstract 3955.

Walsh, G., & Charman, W. (1989). The effect of defocus on the contrast and phase of the retinal image of a sinusoidal grating. *Ophthalmic and Physiological Optics, 9,* 398–404. [PubMed] [Article]

Woods, R., Bradley, A., & Atchison, D. (1996). Monocular diplopia caused by ocular aberrations and hyperopic defocus. *Vision Research, 36,* 3597–3606. [PubMed] [Article]

Yellott, J. I., & Yellott, J. W. (2007). Correcting spurious resolution in defocused images. *Proceedings of SPIE, 6492,* 64920O. [Article]

Zhang, L., & Cottrell, G. W. (2004). *Seeing blobs as faces or letters: Modeling effects on discrimination*. Paper presented at the Proceedings of the 2004 International Conference on Development and Learning, La Jolla, CA.

Zhang, X., Ye, M., Bradley, A., & Thibos, L. (1999). Apodization by the Stiles–Crawford effect moderates the visual impact of retinal image defocus. *Journal of the Optical Society of America A, 16,* 812–820. [PubMed] [Article]